The Pseudoparticulate Expansion of Screen-Packed Gas-Fluidized Beds

C. E. CAPES and A. E. McILHINNEY

National Research Council, Ottawa, Canada

A study has been made of the expansion characteristics of beds of uniformly sized spherical particles of lead, nickel, sand, glass, and plastic that have been fluidized with air, carbon dioxide, and helium in columns packed with open-ended cylindrical screen packing. The addition of packing to a gas-fluidized bed limits the bubble size, prevents slugging and allows beds of high aspect ratio to expand smoothly in a manner similar to the behavior of liquid-fluidized beds. Moreover, much of the experimental data for gas-fluidized screen-packed beds have yielded straight lines on a Richardson-Zaki type of plot, again similar to the expansion of liquid-fluidized beds. The conditions necessary for this pseudoparticulate behavior in packed gas-fluidized beds are discussed. A correlation, based on the analysis given by Richardson and Zaki for liquid-fluidized beds, is proposed to relate bed porosity with gas velocity, density and viscosity, particle size and density, and bed diameter.

Customarily, the spectrum of fluidization behavior is divided into two broad areas described by the terms *particulate* and *aggregative*. Particulate fluidization is distinguished by the regular continuous expansion of a bed of particles as the fluid velocity is increased above the minimum fluidizing velocity to the terminal falling velocity of the particles. Very little fluctuation in bed height is observed. In aggregative fluidization only a limited bed expansion is observed as the fluidizing velocity is raised before some of the fluid begins to pass through the bed as bubbles. A two phase (bubbles and continuous phase) turbulent system results in which wide fluctuations in bed height are observed.

Normally aggregative and particulate behavior results when gases and liquids, respectively, are used for fluidization. There is ample evidence, however, to show that no definite demarcation between the behavior of gas and liquid-fluidized systems exists. Aggregative behavior has been observed when dense solids are fluidized by liquids (*1, 2*) while particulate fluidization may result when solids are fluidized by gases under pressure (*1, 3*) and in gas-fluidized beds which contain baffles and fixed packing (*4, 5*). In addition a number of very finely divided solids that are fluidized with gas at normal pressures give rise to particulate behavior over a limited range of velocities, just above the minimum fluidizing velocity. Such systems have recently been used in the study of the rate of growth of gas bubbles injected into the bed (*6*). Attempts have been made to give criteria for predicting the type of fluidization which can be expected in a given situation. Considerations of the stability of bubbles in a fluidized bed by Harrison, et al. (*2*) have shown that only very small bubbles are normally stable in liquid-solid systems while much larger bubbles can exist in gas-solid systems. The work of Jackson (*7, 8*) complements that of Harrison, et al. (*2*) by showing that small disturbances in the distribution of particles in a fluidized bed will grow as they rise through the bed. The rate of growth is generally small in liquid-fluidized systems leading to smooth fluidization. The rate of growth is generally much larger in gas-solid systems leading to aggregative behavior.

The difference between gas-solid and liquid-solid systems is further emphasized by the lack of a generally applicable correlation between bed voidage, ϵ, and fluid flow-rate, u, for gas-solid systems (*9*). By contrast the expansion of most liquid-fluidized systems of fairly closely-sized particles can be represented by the relationship given by Richardson and Zaki (*10*):

$$\frac{u}{u_o} = \epsilon^n \qquad (1)$$

where n for large tubes is a function only of the particle Reynolds number under free falling conditions. There are indications in the literature that the expansion of systems other than liquid-solid which show particulate behavior may also be represented by Equation (1). Recently, Davies and Richardson (*6*) reported that the expansion of a gas-solid fluidized bed of fine particles with gas rates between the minimum fluidizing velocity, and the minimum velocity at which bubbles are formed, follows a law which is very similar to Equation (1). Leva (*11*) notes that the expansion data of Massimilla and Bracale (*5*) for gas-fluidized beds of glass spheres that contain disks of wire mesh mounted in a series vertically on a central shaft may be represented by an equation of the form of (1), although porosities up to about only 0.65 were measured. In general, however, there is little reported information on the applicability of Equation (1) to other than liquid-fluidized beds. Consequently, our purpose was to determine if the analysis developed by Richardson and Zaki (*10*) for liquid-fluidized systems may be used to correlate the expansion characteristics of packed gas-fluidized beds. A systematic investigation is reported of the expansion, over a wide range of porosities, of beds of uniformly sized

spherical particles of several materials fluidized by various gases under normal pressures and containing cylindrical screen packing. This type of random packing occupies only a small proportion of the bed volume and studies (*4, 12, 13*) have suggested that it should have useful applications in encouraging particulate behavior in gas-fluidized beds of free flowing materials.

EXPERIMENTAL APPARATUS AND PROCEDURE

Four fluidization columns were used in this study. They were 2, 4, 6½, and 12 in. I.D. and their lengths were, respectively, 6, 3, 3, and 5 ft. The first three columns were made from thick walled plastic tube while the largest column was fabricated from stainless steel sheet and had a vertical slot sight glass up its side. A schematic diagram of the layout of the apparatus is shown in Figure 1.

The packing pieces were all formed by rolling rectangles of steel screen into open ended cylindrical shapes. The packing was dumped in small increments into the column and assumed a random arrangement. The properties of the packings used in the study are listed in Table 1. The fluidized solids consisted of various size ranges of glass, silica sand, Gelva (polyvinylacetate), nickel, and lead particles prepared by repeated screening between adjacent Tyler sieves. The particles were all spherical except for the sand which was somewhat angular but rounded and hence was only approximately spherical. One very angular sand was used for some runs in the 12 in. diam. and in the 4 in. diam. column. Most of the runs used air metered by rotameters as the fluidizing gas. In addition a limited number of tests using carbon dioxide and helium as the fluidizing gases were performed. The carbon dioxide and the helium were supplied from cylinders. All the runs were done at a bed temperature of 25°C.

In the case of the Gelva, glass, and sand particles, especially with the smaller sizes, considerable sticking of the charge to the sides of the column was encountered due to electrostatic forces. A hanging-up of the particles due to electrostatic forces was apparent from the considerable reduction in bed pressure drop as the fluidizing velocity was raised. These difficulties were overcome by ensuring that the fluidizing gas had a relative humidity of about 35% with the glass and sand particles, and about 50% with the Gelva beads. Moisture was added to the gases by bubbling them through water and in the case of air by using a Nash compressor, which allows control of the moisture content of the compressed gas.

In a typical run the packing was poured into the column to a height slightly greater than that of the particulate bed at incipient fluidization. Then a known weight of bed was added followed by sufficient packing to allow for a six or sevenfold expansion. A ratio of H_{mf}/D approximately equal to 2 or 4 was maintained during the runs. To measure the expansion, the gas flow was increased until fluidization definitely occurred and then it was decreased incrementally into the fixed bed region with pressure drop and bed height being noted. The gas flow rate was then increased to fluidization level and again increased incrementally to maximum conditions. This procedure was adopted to avoid excessive pressure drop in the quiescent bed range because of settling and to minimize the effect of any solids hold up in the packing over the fluidization range.

Table 1. Properties of Cylindrical Screen Packing

Mesh size of screen	Wire thickness in.	Dimensions of opening in.	Dimensions of screen cylinders in.	Volume not occupied by wire per unit volume of packing in 2 in. column	4 in. column	6½ in. column	12 in. column
4	0.023	0.228 × 0.228	½ × ½	0.975	0.970	0.971	—
6	0.035	0.130 × 0.130	¾ × ¾	—	—	—	0.961
8	0.015	0.106 × 0.106	½ × ½	0.974	0.970	0.961	—
14	0.018	0.051 × 0.051	½ × ½	0.951	—	—	—

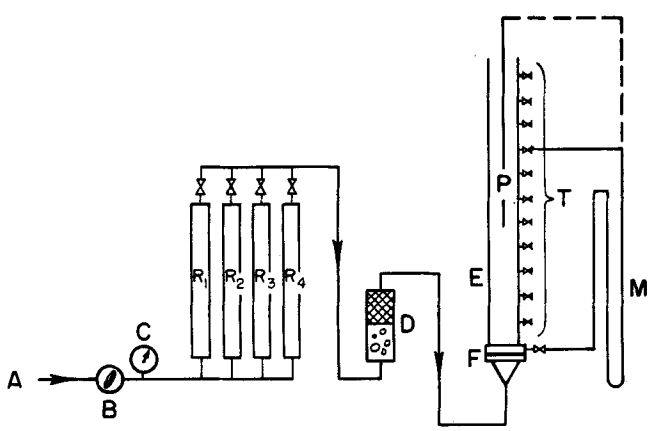

Fig. 1. Layout of fluidization apparatus. A. gas from Nash compressor or cylinders; B. pressure controller; C. pressure gauge; D. gas humidifier; E. fluidization column; F. gas distributing plate; M. manometer; P. pressure probe, T. pressure taps (P & T—alternative ways to measure pressure profiles); R_1, R_2, R_3, R_4, rotometers.

RESULTS AND DISCUSSION

Expansion Curves

The bulk of the experimental measurements of bed expansion were done with lead, nickel, glass, sand, and Gelva particles fluidized with air in the 2 in. diam. column containing various cylindrical screen packings. As in previous studies (*9, 10*), bed weight was found to have no significant effect on the expansion data, and normally bed weights of 500 g. of glass or sand particles, 1,500 g. of nickel or lead particles and 200 g. of Gelva beads were used in the 2 in. diam. column. Throughout this work, allowance was made for the tube volume occupied by the packing, based on the data given in Table 1. That is, the bed voidage was calculated as the ratio

$$\frac{\text{volume of tube} - \text{volume of packing} - \text{volume of particles}}{\text{volume of tube} - \text{volume of packing}}$$

while the superficial gas velocity was based on the cross-sectional area of the tube not occupied by packing.

Experimental results are shown in Figures 2, 3, and 4 as a plot of bed voidage vs. superficial gas velocity using a log-log scale. It is evident from Equation (1) that expansion curves for particulately fluidized beds on this type of plot should be linear. Examination of Figures 2 to 4 shows that gas-fluidized screen-packed beds of uniformly sized particles yield linear expansion curves provided the particle size is equal to, or greater than, about 28/32 Tyler mesh (545 μ). With smaller particles, nonlinear curves result and the beds show less expansion than would be expected with a linear expansion curve intercepting the $\epsilon = 1$ axis at the particle terminal velocity. It should also be noted that the particle size, with which the expansion curves become nonlinear, is independent of particle density and of screen packing mesh size; although the degree of

curvature is apparently dependent on the screen packing mesh size. Sutherland, et al. (*4*) previously studied the expansion characteristics of fluidized beds containing the same packing used here and concluded that the expansion curves could not be represented by an equation such as (1). However, most of their work was done with sand and glass particles smaller than 28/32 Tyler mesh and, in agreement with the findings of the present investigation, would be expected to yield nonlinear expansion curves.

From the plots given in Figures 2 to 4, it may be stated that the presence of screen packing causes gas-fluidized beds of particles larger than about ½ mm. in diameter to expand in a manner similar to liquid-fluidized beds, while beds of smaller particles expand in the same way as has previously been reported for conventional gas-fluidized beds (*9, 11*). It has been suggested (*9, 11, 14*) that the difference in expansion behavior between gas- and liquid-fluidized beds is due to differences in particle motion and energy losses in the beds caused by bubbles. The addition of screen packing to gas-fluidized beds constrains particle motion (*4, 15*), bubble size and rate of growth are limited, and behavior more closely approaching that of a particulately-fluidized bed is observed.

The finding that the particle size with which the expansion curves changed from linear to nonlinear is independent of packing properties is rather surprising. As seen in Table 1, the openings in the screen used to make the cylindrical packing varied considerably. One might therefore expect the degree of constraint imposed by the different packings and hence the expansion behavior of the packed fluidized beds to be dependent on packing properties. However, a study by Lochiel and Sutherland (*16*) of the circulation rate of particles through screens which subdivided a gas-fluidized bed suggests that the fractional

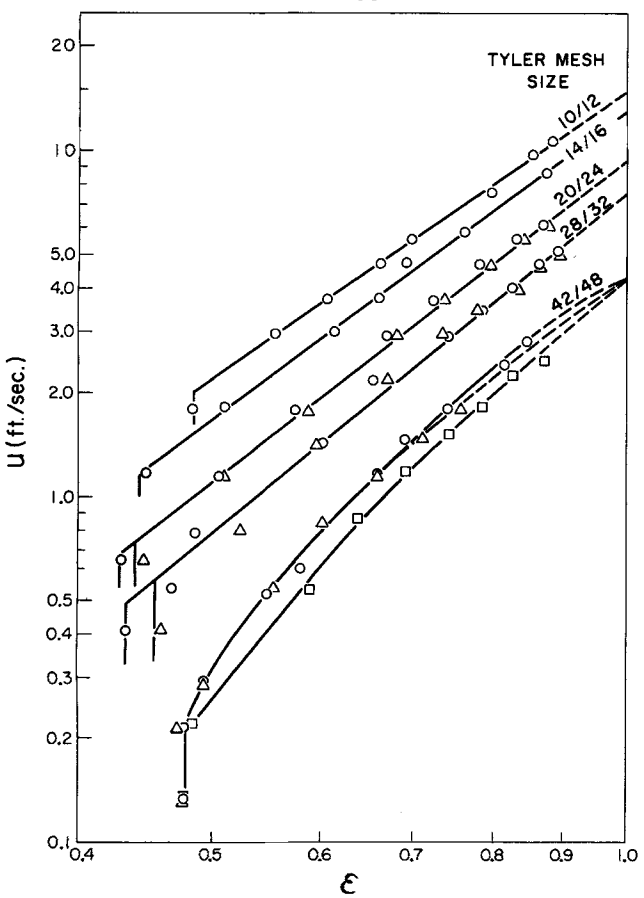

Fig. 2. Fluidization of gelva beads with air in 2 in. column.
○ 4 mesh ½ in. × ½ in. screen cylinders.
△ 8 mesh ½ in. × ½ in. screen cylinders.
□ 14 mesh ½ in. × ½ in. screen cylinders.

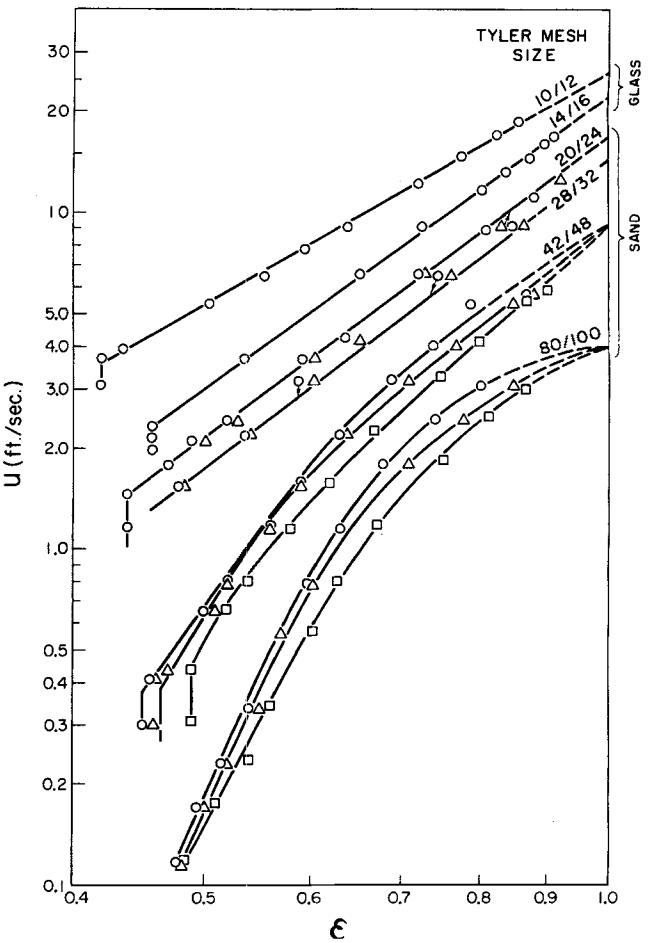

Fig. 3. Fluidization of sand and glass beads with air in 2 in. column. See Figure 2 for key to symbols.

free volume of the packings is the property which determines the degree of constraint placed on the particles. As is seen in Table 1, the fractional free volume of the packings used varied only slightly leading to expansion behavior essentially independent of which packing was used.

The lower limit of particle size, for which linear expansion curves are obtained, occurs when the particles are so small that the packing no longer sufficiently restrains their movement. An upper limit of particle size which is possible to use in screen-packed beds is reached when the packing impedes particle circulation too severely, and the particles begin to hang-up on the packing. Under these conditions, the gas flows in channels through the bed, and the pressure drop is reduced below the theoretical value based on the total weight of solids. Experience in this laboratory indicates that the ratio of mesh opening to particle size should be greater than about 3 or 4 to allow the particles to flow freely through the packing. Hence 10/12 Tyler mesh particles in combination with the 4 mesh packing were the largest particles that it was possible to use in the present investigation.

Effect of Column Diameter

In addition to the experiments carried out in the 2 in. I.D. column already discussed, a number of expansion runs were performed with the lead, nickel, glass and sand particles fluidized in 4, 6½, and 12 in. I.D. columns. As discussed earlier, the maximum particle size that was possible to use was 15.5×10^{-2} cm. (10/12 Tyler mesh), which corresponds to a maximum value of the ratio of particle diameter to column diameter (d/D) of about 3×10^{-2}. Representative results of these experiments are shown in Figure 5 where it is seen that the column diame-

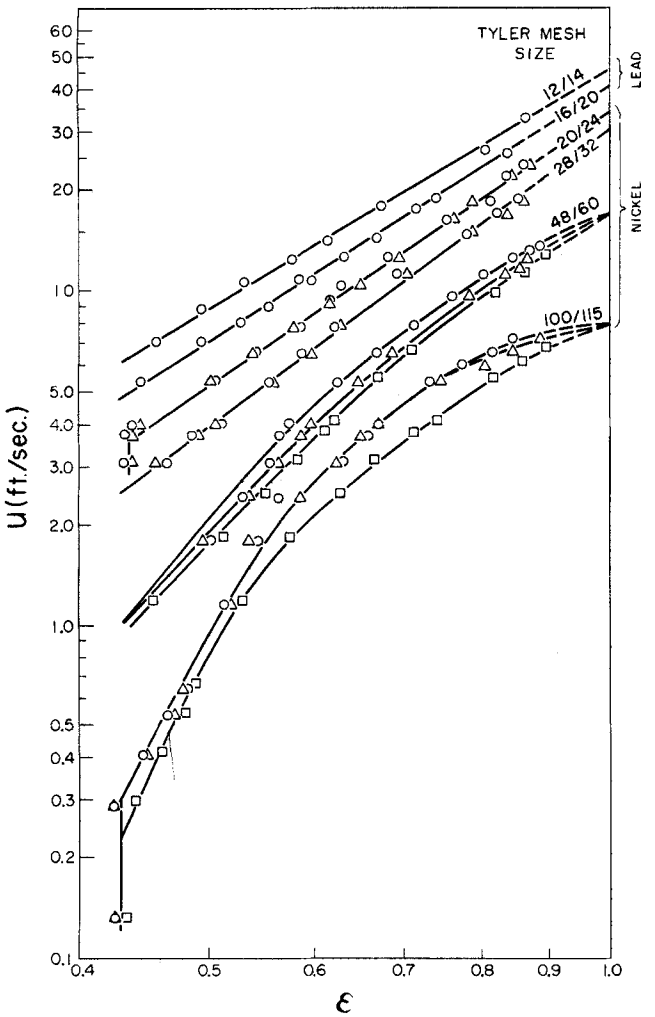

Fig. 4. Fluidization of nickel and lead shot with air in 2 in. column. See Figure 2 for key to symbols.

ter has no significant effect on the expansion curves for the range of variables studied. This conclusion may be compared with that reached by Richardson and Zaki (*10*) in their study of the sedimentation and fluidization of particles in liquids. During sedimentation, the value of the falling velocity of the suspension extrapolated to $\epsilon = 1$ agreed with the terminal falling velocity of the particles in an infinite medium whereas during fluidization the comparable extrapolated value of the fluid velocity was normally less than the particle terminal falling velocity in an infinite medium. The difference became greater as the value of d/D increased. In other words, as d/D increased the porosity of the fluidized bed was higher with other conditions being the same (*17*). This difference was attributed (*10*) to the fact that in fluidization a velocity gradient is created in the liquid because of the drag exerted by the walls.

Two reasons for the absence of any significant effect due to column diameter in the present work may be suggested. Firstly, the maximum value of d/D which it was possible to use [3×10^{-2} compared with the value of 11×10^{-2} used by Richardson and Zaki (*10*)] may not have been sufficiently large for the effect to be apparent. Secondly, it should be realized that the screen packing divides the column into a large number of tortuous flow paths of diameter smaller than the size of the packing pieces and only a few times larger than the particles. Any effect exerted by the column walls might therefore be expected to be insignificant compared with that caused by the screen packing whose structure is independent of column diameter.

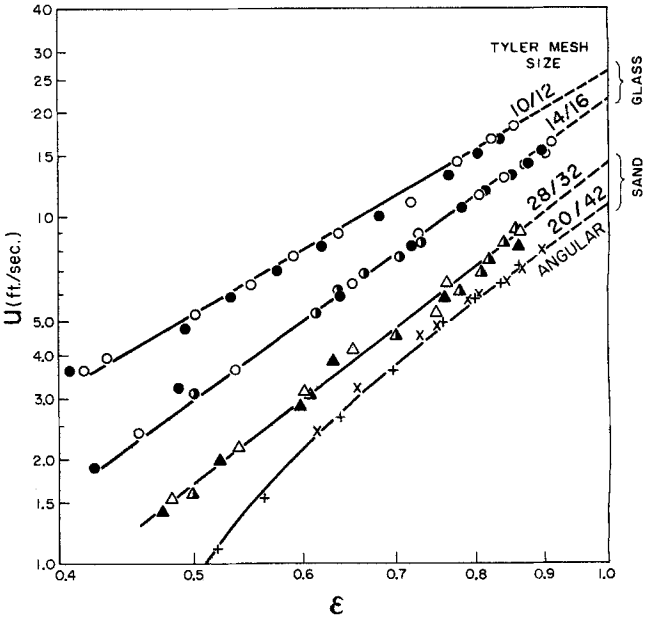

Fig. 5. Fluidization of sand and glass beads with air in 2, 4, 6½, and 12 in. columns.

Column Diameter:	2 in.	4 in.	6½ in.	12 in.
Screen Packing:				
4 mesh, ½ in. × ½ in.	○	●	◑	
8 mesh, ½ in. × ½ in.	△	▲	◭	
6 mesh, ¾ in. × ¾ in.		+		×

Correlation of Results

Since it has been shown that sufficiently large particles gas-fluidized in beds of screen packing yield expansion curves similar to those of liquid-fluidized particles, it is reasonable to expect to be able to correlate this expansion data by the method developed by Richardson and Zaki (*10*) for liquid-fluidized beds. Toward this end, expansion curves for lead and nickel particles fluidized by carbon dioxide (Figure 6) and for Gelva beads fluidized by helium (Figure 7) were determined to extend the data to, respectively, higher and lower particle Reynolds numbers than are possible in the corresponding air-fluidized systems.

The linear expansion curves may be represented by the equation

$$\frac{u}{u_i} = \epsilon^n \qquad (2)$$

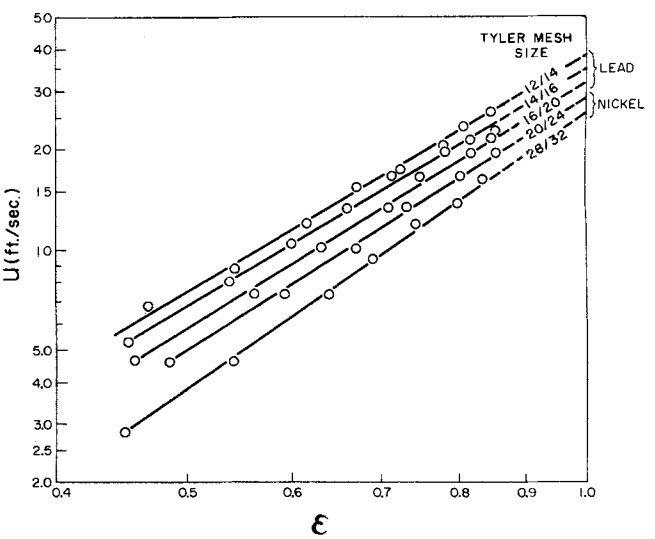

Fig. 6. Fluidization of nickel and lead shot with carbon dioxide in 2 in. column. 4 mesh, ½ in. × ½ in. screen cylinders.

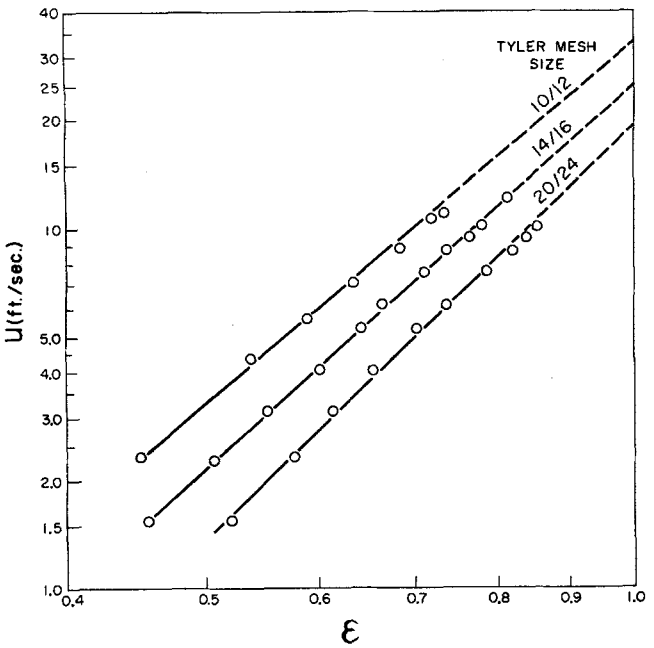

Fig. 7. Fluidization of gelva beads with helium in 2 in. column. 4 mesh, ½ in. × ½ in. screen cylinders.

where n is the slope of the log-log curve and u_i is the value of u extrapolated to $\epsilon = 1$.

As indicated in Figure 5, it is assumed that d/D has no effect on bed expansion for the range of conditions of interest here. The dimensional analysis given by Richardson and Zaki (*10*) applied to screen-packed beds yields the result

$$n = f_1\,(N_{Re_o}\text{ only}) \tag{3}$$

and

$$\frac{u_i}{u_o} = f_2\,(N_{Re_o}\text{ only}) \tag{4}$$

Provided either the viscous or the inertial forces can be neglected, Equations (3) and (4) become

$$n = a \quad \text{constant} \tag{5}$$

and

$$\frac{u_i}{u_o} = a \quad \text{constant} \tag{6}$$

The slopes, n, and the intercepts u_i, of the linear expansion curves in Figures 2 to 7 are given in Table 2 together with the corresponding values of u_o, u_o/u_i and N_{Re_o}. The terminal falling velocities of the particles in an infinite medium were calculated using the tables compiled by Heywood (*18*) from literature data. The values of the slope n and the ratio u_o/u_i are plotted in Figure 8 as a function of N_{Re_o}.

TABLE 2. SUMMARY OF EXPERIMENTAL RESULTS

PARTICLES				GAS (25°C)			FROM LOG-LOG PLOT OF u VERSUS ε				
	Size		Density		Density	Viscosity	u_o	Re_o	u_i	Slope	u_o/u_i
Material	Tyler Mesh	cm.	gm/cu.cm.		gm/cu.cm.	centipoises	ft/sec		ft/sec		
Gelva Beads	10/12	15.45×10^{-2}	0.958	Air	1.175×10^{-3}	0.018	17.46	538	14.9	2.76	1.17
"	14/16	10.95×10^{-2}	"	"	"	"	13.56	296	12.8	2.97	1.06
"	20/24	7.75×10^{-2}	"	"	"	"	9.93	153	9.43	3.11	1.05
"	28/32	5.45×10^{-2}	"	"	"	"	7.0	76.4	7.44	3.26	0.94
Glass Beads	10/12	15.45×10^{-2}	2.73	Air	1.175×10^{-3}	0.018	32.3	995	26.3	2.28	1.23
"	14/16	10.95×10^{-2}	"	"	"	"	25.1	548	22.1	2.91	1.14
Sand	20/24	7.75×10^{-2}	2.67	"	"	"	19.1	294	17.0	2.98	1.12
"	28/32	5.45×10^{-2}	"	"	"	"	13.9	153	14.4	3.04	0.96
Lead Shot	12/14	13.0×10^{-2}	11.34	Air	1.175×10^{-3}	0.018	64.4	1672	46.0	2.36	1.40
"	14/16	10.95×10^{-2}	"	"	"	"	57.4	1252	41.4	2.41	1.39
"	16/20	9.20×10^{-2}	"	"	"	"	50.7	931	40.5	2.53	1.25
Nickel	20/24	7.75×10^{-2}	8.90	"	"	"	38.9	600	34.7	2.75	1.12
"	28/32	5.45×10^{-2}	"	"	"	"	29.6	322	30.1	2.96	0.98
Lead Shot	12/14	13.0×10^{-2}	11.34	Carbon dioxide	1.841×10^{-3}	0.0146	53.8	2690	38.0	2.37	1.42
"	14/16	10.95×10^{-2}	"	"	"	"	48.2	2030	34.6	2.40	1.39
"	16/20	9.20×10^{-2}	"	"	"	"	43.0	1519	31.8	2.46	1.35
Nickel	20/24	7.75×10^{-2}	8.90	"	"	"	33.4	993	28.0	2.52	1.19
"	28/32	5.45×10^{-2}	"	"	"	"	25.9	543	25.5	2.77	1.02
Gelva Beads	10/12	15.45×10^{-2}	0.958	Helium	0.1663×10^{-3}	0.0188	36.9	152	33.2	3.33	1.11
"	14/16	10.95×10^{-2}	"	"	"	"	26.8	79	25.5	3.57	1.05
"	20/24	7.75×10^{-2}	"	"	"	"	19.5	41	19.6	3.84	0.99

At Reynolds numbers greater than about 1,400, corresponding to the conditions under which viscous forces are negligible, n and u_o/u_i are independent of N_{Re_o} in agreement with Equations (5) and (6). That is, for $N_{Re_o} > 1{,}400$,

$$n = 2.37 \tag{7}$$

$$\frac{u_o}{u_i} = 1.38 \tag{8}$$

At Reynolds numbers less than about 1,400, n and u_o/u_i are both dependent upon N_{Re_o} and may be represented by the equations

$$N_{Re_o} < 1{,}400,\ \frac{u_o}{u_i} = 0.96 + 3.04 \times 10^{-4}\, N_{Re_o} \tag{9}$$

$$150 < N_{Re_o} < 1{,}400,\ n = 3.16 - 5.72 \times 10^{-4}\, N_{Re_o} \tag{10}$$

$$N_{Re_o} < 150,\ n = 3.98 - 6.00 \times 10^{-3}\, N_{Re_o} \tag{11}$$

The value $n = 2.37$ for the slope of the expansion curve when viscous forces are negligible agrees well with the value $n = 2.39$ found by Richardson and Zaki (*10*) for liquid-fluidized beds. In liquid fluidization, however, viscous forces become negligible for Reynolds numbers greater than about 500 (see curve in Figure 8) whereas in the present work the corresponding value was $N_{Re_o} = 1{,}400$. This difference is attributable to the fact that fine mesh screens may be used to reduce turbulence in an air stream (*19*) and is compatible with the work of Chen and Osberg (*20*) on radial gas dispersion in a column packed with screen cylinders, in which the wire packing was found to suppress turbulent diffusion compared with that in an empty tube.

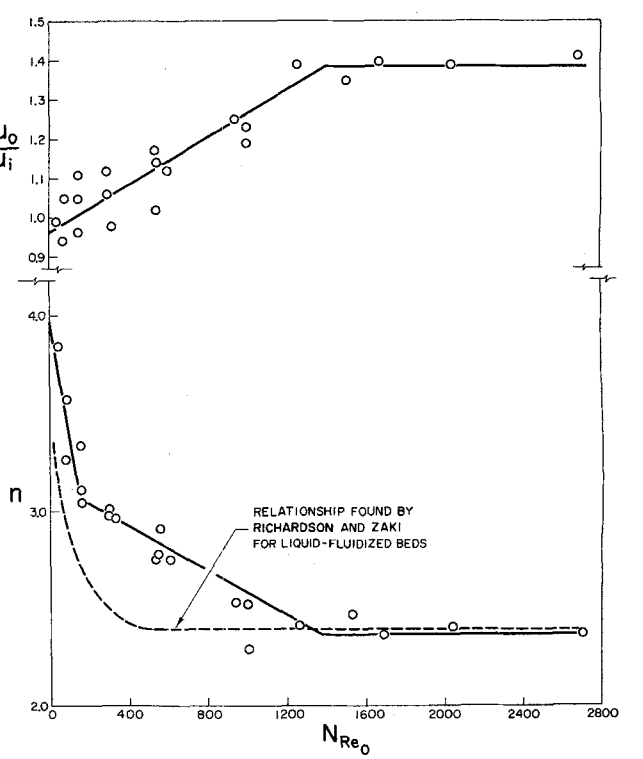

Fig. 8. Slope n and ratio u_o/u_i as a function of N_{Re_o}.

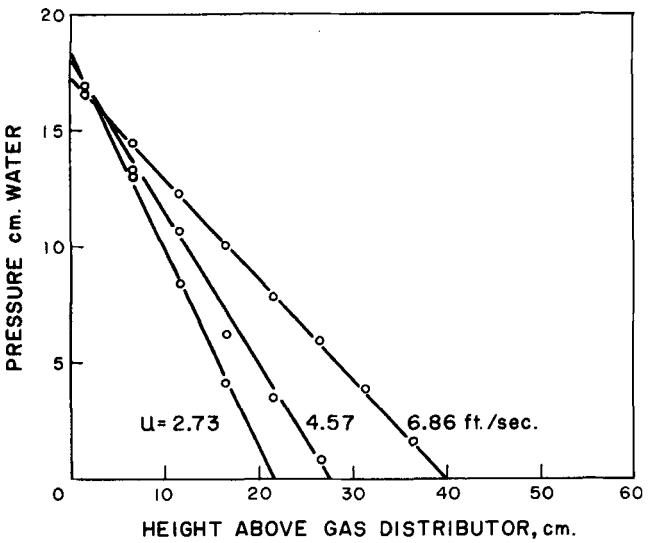

Fig. 9. Pressure profiles up wall of 2 in. column for various superficial air velocities. Pressure at top of bed = 0 cm. water. 20/24 mesh sand particles, 4 mesh, ½ in. × ½ in. packing.

The Character of the Fluidized Bed

The expansion data presented above suggests that large particles gas-fluidized in a screen-packed bed show true particulate behavior. In addition, the pressure profiles measured up the center of a 12 in. diam. bed and up the wall of a 2 in. diam. bed (Figure 9) were found to be linear; this indicates that bed density is constant with height as would be expected for a uniform dispersion of solid and fluid. By contrast a conventional gas-fluidized bed can be divided into at least two layers, a first relatively dense layer from the bed support up to the height of the bed at incipient fluidization and a second relatively dilute layer above this height (*21*).

Examination of these gas-fluidized screen-packed beds of large particles shows, however, that a uniform dispersion of solid and fluid does not prevail. Relatively large gas pockets or voids are evident, especially at the higher voidages when less active groups of particles collect downstream of the packing pieces and drain through the openings in the screen cylinders. Therefore on a large scale these beds are particulate in nature as evidenced by, for example, the expansion curves and vertical pressure profiles while on a smaller scale the beds are not particulate in the sense that the particles are not supported individually and are not dispersed uniformly in the fluid. The behavior of these screen-packed beds may thus best be described as "pseudoparticulate."

CONCLUSIONS

Cylindrical screen packing limits the size and rate of growth of bubbles in gas-fluidized beds by constraining particle movement. As a result, the expansion of beds of relatively large particles gas-fluidized in columns that contain this packing may be represented by the same equation which has been used to describe the expansion of liquid-fluidized beds, namely:

$$\frac{u}{u_i} = \epsilon^n$$

For the screen packing used in the present study, n and u_i are given by Equations (7) to (11) inclusive. The correlation represents data for particles equal to or greater than 28/32 Tyler mesh ranging in density from that of plastic (0.96 g./cc.) to lead (11.3 g./cc.) fluidized by air, carbon dioxide, and helium in columns ranging in diameter from 2 to 12 in. The behavior of the beds whose expansion is represented by this correlation is not truly particulate, however, since relatively large pockets of gas exist within them so that the fluid-solid mixture is not homogeneous.

Particles finer than 28/32 Tyler mesh are less constrained in their movement and yield nonlinear expansion curves. There is evidence that the fractional free volume is the property of the packing which determines the degree of constraint placed on the motion of particles fluidized in it.

ACKNOWLEDGMENT

The authors thank Dr. G. L. Osberg and Dr. W. K. Kang for helpful discussion and J. P. Kolody for help with various aspects of the investigation.

NOTATION

d = particle diameter, cm.
D = column diameter, cm.
H_{mf} = bed height at minimum fluidizing velocity, cm.
n = slope obtained from plot of log u vs. log ϵ
N_{Re_o} = $u_o d\rho/\mu$ = particle Reynolds number under free falling conditions
u = superficial gas velocity, ft./sec.
u_o = terminal falling velocity of a single particle, ft./sec.
u_i = extrapolated value of u at $\epsilon = 1$, ft./sec.
ϵ = porosity
μ = fluid viscosity, centipoise
ρ = fluid density, g./cc.

LITERATURE CITED

1. Simpson, H. C., and B. W. Rodger, *Chem. Eng. Sci.*, **16**, 153 (1961).
2. Harrison, D., J. F. Davidson, and J. W. de Kock, *Trans. Inst. Chem. Engrs. (London)*, **39**, 202 (1961).
3. Leung, L. S., Ph.D. thesis, Univer. Cambridge, England (1961).
4. Sutherland, J. P., G. Vassilatos, H. Kubota, and G. L. Osberg, *AIChE J.*, **9**, 437 (1963).
5. Massimilla, L., and S. Bracale, *Ric. Sci.*, **26**, 487 (1956).
6. Davies, L., and J. F. Richardson, *Trans. Inst. Chem. Engrs. (London)*, **44**, 293 (1966).
7. Jackson, R., *ibid.*, **41**, 13 (1963).
8. Anderson, T. B., and R. Jackson, *Chem. Eng. Sci.*, **19**, 509 (1964).
9. Davies, G., and D. B. Robinson, *Can. J. Chem. Eng.*, **38**, 175 (1960).
10. Richardson, J. F., and W. N. Zaki, *Trans. Inst. Chem. Engrs. (London)*, **32**, 35 (1954).
11. Leva, M., "Fluidization," McGraw-Hill, New York (1959).
12. Ishii, T., G. L. Osberg, *AIChE J.*, **11**, 279 (1965).
13. Capes, C. E., and J. P. Sutherland, *Ind. Eng. Chem. Process Design Develop.*, **5**, 330 (1966).
14. Othmer, D. F., ed., "Fluidization," p. 14, Reinhold Pub. Corp., New York (1956).
15. Massimilla, L., and J. W. Westwater, *AIChE J.*, **6**, 134 (1960).
16. Lochiel, A. C., and J. P. Sutherland, *Chem. Eng. Sci.*, **20**, 1041 (1965).
17. Neuzil, L., and M. Hrdina, *Collection Czech. Chem. Commun.*, **30**, 752 (1965).
18. Heywood, H., *Symp. Interaction between Fluids Particles*, p. 1, *Inst. Chem. Engrs. (London)* (1962).
19. Dryden, H. L., and G. B. Shubauer, *J. Aero. Sci.*, **14**, 221 (1947).
20. Chen, B. H., and G. L. Osberg, *Can. J. Chem. Eng.*, **45**, 46 (1967).
21. Bakker, P. J., and P. M. Heertjes, *Chem. Eng. Sci.*, **12**, 260 (1960).

Manuscript received January 30, 1967; revision received January 5, 1968; paper accepted January 10, 1968. Paper presented at AIChE New York City meeting.